Sulfonation of Surface-Initiated Polynorbornene Films

Brad J. Berron, P. Andrew Payne, and G. Kane Jennings*

Department of Chemical Engineering, Vanderbilt University, Nashville, Tennessee 37235

We report the sulfonation of surface-initiated polynorbornene with acetyl sulfate to produce ultrathin ionomer films. The complete process consists of exposure of a hydroxyl-terminated self-assembled monolayer (SAM) on gold to a norbornenyl diacid chloride, attachment of Grubbs first generation catalyst, ring-opening metathesis polymerization (ROMP), and sulfonation. Structural and chemical changes in the film upon sulfonation are confirmed by RAIRS, contact angle goniometry, ellipsometry, optical microscopy, and electrochemical impedance spectroscopy. Sulfonation of surface-initiated polynorbornene results in a highly nonuniform surface morphology which can be relaxed to a more uniform film through exposure to dimethyl sulfoxide at room temperature. The sulfonated polynorbornene films have an intermediate surface energy ($\theta_A(H_2O) \approx 75°$) and a low resistance against proton transport ($R_f \approx 1.6\ \Omega \cdot cm^2$), which is 6 orders of magnitude lower than that of the original polynorbornene film. The sulfonated films are far more stable than the original polynorbornene films because of a ~95% diminution of olefin content within the film. Sulfonated poly(butylnorbornene) films were prepared analogously to demonstrate the versatility of this approach toward ionomer films.

Introduction

The unique chemical behavior of sulfonated polymer films has made them of particular interest in modern technologies. Sulfonated polymers are well established as the standard in proton exchange media for fuel cells.[1−5] These polymers are commonly prepared as thick films by solution casting,[6−8] a method that is inadequate to achieve conformal coatings on irregular substrates that are becoming utilized as fuel cell architectures evolve.[7,9−12] Sulfonated polymers are also useful in ion exchange applications including water purification and desalination.[13,14] Alternative sulfonated polymeric structures are of relevance given the increasing research interest in efficiently extracting water from saltwater sources.[13]

The abundance of naturally occurring biopolymers which include or interact with sulfonate functionality suggests the promise that sulfonated polymer surfaces hold for applications as biomimetic materials. Eckenrode and Dai recently highlighted the ability for sulfonated polystyrene surfaces to adsorb positively charged polylysine.[15] The biological adsorption of charged molecules has shown to play a key role in immunoadsorption as well as blood clotting.[16] Huck and co-workers recently reported the application of silver-loaded poly(3-sulfopropylmethacrylate) films as an antibacterial surface.[17] The ion exchange properties of new types of sulfonated polymer surfaces as well as the ability to incorporate these films into more complex architectures should continue to drive the development of the next generation of biomaterials.

Surface-initiated polymerization offers advantages over spin coating and solution casting owing to a chemisorbed linkage of the polymer to the surface,[18−23] the ability to conformally coat substrates of any geometry,[18,24,25] and the exceptional film uniformity at a low film thickness.[21,26−28] Surface-initiated films with sulfonate functionality are typically prepared through the growth and sulfonation of polystyrene.[29,30] Alternatively, the growth and sulfonation of polynorbornene films would be advantageous because they are grown rapidly through ring-opening metathesis polymerization (ROMP), yielding an 80 nm film after 15 min of polymerization at room temperature.[31] In contrast, almost 36 h at temperatures in excess of 75 °C are required to grow polystyrene films of comparable thickness.[29,30] The surface-initiated polymerization of a sulfonate-containing monomer via atom transfer radical polymerization (ATRP) also has slow polymerization rates when compared to ROMP, requiring over 5 h to grow an 80 nm film.[17,32] The tailorable functionality of norbornene-based monomers allows for a variety of modified ROMP-type films to be sulfonated via an analogous approach.[33]

Here, we demonstrate the growth and sulfonation of surface-initiated polynorbornene films. Our approach is outlined in Figure 1. An alcohol-terminated self-assembled monolayer (SAM) (Au/SC_4OH) is prepared by exposure of a gold-coated silicon substrate to 1-mercapto-4-butanol. The alcohol-terminated monolayer is then reacted with a diacidchloride-functionalized norbornene ($NB(COCl)_2$) to tether the norbornenyl group to the surface via ester linkages. Exposure to Grubbs first

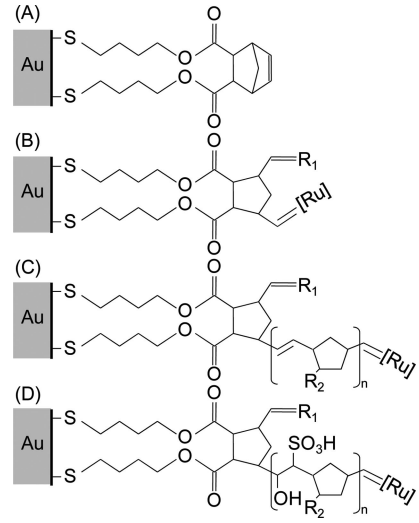

Figure 1. Schematic illustration of the preparation of sulfonated films by attachment of a norbornenyl decorated SAM (A), attachment of Grubbs' catalyst (B), the ring-opening metathesis polymerization of norbornene (C), and the sulfonation of the surface tethered film with acetyl sulfate (D). [Ru] = $(PCy_3)_2Cl_2Ru$, Cy = cyclohexyl. R_1 = CHPh. R_2 = −H for polynorbornene, $-(CH_2)_3CH_3$ for poly(butylnorbornene).

* To whom correspondence should be addressed. E-mail: kane.g.jennings@vanderbilt.edu.

10.1021/ie800356a CCC: $40.75
Published on Web 09/18/2008

generation catalyst results in a submonolayer of immobilized ROMP-active catalyst.[24] The bound catalyst is then reacted with the appropriate norbornene (NB) monomer, resulting in a surface-tethered ROMP-type polymer film, which is then sulfonated by exposure to freshly prepared acetyl sulfate. The immobilization of an acid chloride-functionalized norbornene on a hydroxyl-terminated monolayer is a fast and convenient method for achieving a norbornenyl-decorated surface through the sequential exposure to commercially available materials. This approach allows techniques based on SAMs to control the nature of the linkage of the polymer to the underlying gold support.

The versatility of olefin chemistry offers many reaction pathways for the sulfonation of polynorbornene.[34] Typically, the unsaturated polymer is exposed to an adduct of sulfur trioxide yielding a highly unstable β-sultone. Upon exposure to water, the sultone is rapidly converted to either an olefinic sulfonate or a hydroxylsulfonate.[33,34] The distinction between the products is determined by the nature of the adduct as well as the olefin.[34,35] Previously, Planche et al. have sulfonated solution-phase polynorbornene with the SO_3-triethylphosphate adduct yielding almost exclusively an olefinic sulfonate product.[35,36] In the interest of polymer stability, the persistence of the olefin functionality in the sulfonated product is not desirable. Boyd and Schrock have reported the solution-phase sulfonation reaction of modified polynorbornenes using a SO_3-dioxane adduct.[33] They observed >80% conversion of the olefin as well as selectivity toward the more desirable hydroxylsulfonate product. Dioxane was chosen as a complexing reagent, due to the lack of reactivity of SO_3-dioxane with the aromatic side chains present in their studies.[33] Hoffman and Simchen developed a more convenient preparation of SO_3-dioxane by observing that the addition of dioxane to trimethylsilyl chlorosulfonate yields SO_3−dioxane and chlorotrimethylsilane,[37,38] alleviating the need to use sulfur trioxide as a reagent. The chloromethylsilane byproduct is typically removed by vacuum distillation. Acetyl sulfate is another conveniently prepared, reactive sulfonation reagent achieved by the stoichiometric addition of sulfuric acid to acetic anhydride.[39,40] Acetyl sulfate has been shown to be reactive with olefin functionality to generate a β-sultone[40] and is promising for utility in the sulfonation of polynorbornene.

Here, we investigate the use of acetyl sulfate as a sulfonation reagent for surface-tethered polynorbornene and poly(butylnorbornene) and the applicability of these materials as proton-conducting films. We use reflectance-absorption infrared spectroscopy (RAIRS) to probe the structural and chemical changes during sulfonation. Previously, we demonstrated the uniformity of surface-initiated polynorbornene and poly(butylnorbornene) films.[31] Here, we use optical microscopy to investigate the microscopic changes in film morphology upon sulfonation and further surface treatment. Electrochemical impedance spectroscopy is used to determine the proton transport properties of the films. We have previously reported that surface-initiated polynorbornene films provide excellent resistance to the transport of water and large ions.[31] Upon sulfonation, the sulfonate functionality of the polymer should provide hydrophilic domains in the polymer structure which facilitate proton and water transport through the film. The reorganization of polymers into hydrophobic and hydrophilic domains is known to be vital to proton transport through commercial proton exchange membranes due to a water-mediated proton transport mechanism.[1,3,4]

Experimental Section

Materials. 4-Mercapto-1-butanol (97%), 1-pentanethiol (98%), and Grubbs catalyst−first generation (benzylidene-bis(tricyclohexylphosphine)dichlororuthenium) were used as received from Sigma-Aldrich. Norbornene (NB, 99%) was used as received from MP Biomedicals. 5-*n*-Butylnorbornene (98%) was provided by Promerus Electronic Materials and used as received. *trans*-3,6-Endomethylene-1,2,3,6-tetrahydrophthaloyl chloride (97%), acetic anhydride (99%), dimethyl sulfoxide (99%), dichloromethane (99.9%), and toluene (99.9%) were used as received from Fisher Scientific. Sulfuric acid (95%) was used as received from EM Science. Gold shot (99.99%) and chromium-coated tungsten filaments were obtained from J&J Materials and R.D. Mathis, respectively. Silicon wafers (100) were obtained from Montco Silicon. Ethanol (absolute) was used as received from AAPER. Deionized water (16.7 MΩ·cm) was purified with a Modu-Pure system.

Preparation of Gold Substrates. Silicon wafers were rinsed with ethanol and water and dried in a nitrogen stream. Chromium (100 Å) and gold (1250 Å) were sequentially evaporated onto silicon wafers at rates of <2 Å s^{-1} in a diffusion-pumped chamber with a base pressure of $<5 \times 10^{-6}$ Torr. The wafers were typically cut into sample sizes of 1.5 cm × 3.5 cm.

Polymerization. Gold substrates were placed in a 1.0 mM ethanolic solution of 4-mercapto-1-butanol for at least 60 min to yield a hydroxyl-terminated self-assembled monolayer. The samples were rinsed in ethanol and dried in a stream of nitrogen. Exposure of the SAM to a 5.0 mM solution of *trans*-3,6-endomethylene-1,2,3,6-tetrahydrophthaloyl chloride in dichloromethane for 30 min yields the acylation product of a surface-tethered norbornenyl group. The samples were rinsed in ethanol and dried in a stream of N_2. The norbornenyl decorated substrates were exposed to a 5 mM solution of Grubbs catalyst in dichloromethane for 15 min. The catalyst-coated films were rinsed with dichloromethane and immediately placed in a monomer solution containing 1.0 M norbornene in toluene for 15 min to achieve ~120 nm polymer films. The films were sequentially rinsed with toluene, ethanol, and water and dried in a stream of nitrogen. Poly(*n*-butylnorbornene) films were prepared analogously using a monomer solution containing 1.0 M 5-*n*-buytlnorbornene in dichloromethane.

Sulfonation. A 1.0 M acetyl sulfate solution in dichloromethane was prepared immediately prior to use similar to Tran et al.[39] Acetic anhydride (2.8 mL) was added to dichloromethane (14.0 mL) at 0 °C. Concentrated sulfuric acid (1.0 mL) was added dropwise to the acetic acid solution resulting in a 1.0 M acetyl sulfate solution in DCM. A 1.0 mL aliquot of the 1.0 M acetyl sulfate solution was diluted to 0.1 M through the addition of 9.0 mL of dichloromethane. Polymer-coated substrates were exposed to the 0.1 M solution of acetyl sulfate for 60 s to yield a surface-tethered sulfonated polymer coating. Samples were rinsed with dichloromethane and ethanol and dried in a nitrogen stream. The resulting polymer films were exposed to dimethyl sulfoxide (DMSO) for 5 to 30 min.

Characterization Methods. Film properties were evaluated using the following methods to determine the structure and properties of the films. Reflectance-absorption infrared spectroscopy (RAIRS) was performed using a Varian 3100 FT-IR spectrometer in single reflection mode with a universal sampling accessory and a liquid nitrogen-cooled, narrow-band MCT detector. *p*-Polarized light was incident at 80° from the surface normal. Spectra were collected over 200 scans at a resolution of 2 cm^{-1} using a clean gold-coated silicon wafer as a reference. IR spectra of monolayer films were collected using polarization modulation infrared reflection absorption spectroscopy (PM-IRRAS). Data were collected using a Bruker PMA-50 attach-

ment on a Bruker Tensor 26 infrared spectrometer equipped with a liquid-nitrogen-cooled MCT detector and a Hinds Instruments PEM- 90 photoelastic modulator. The source beam was modulated at a frequency of 50 kHz with half-wavelength retardation and set at 80° incident to the sample surface. Spectra for SAMs on gold substrates were collected over 5 min (380 scans) at a resolution of 4 cm^{-1}. The differential reflection spectra ($\Delta R/R$) were calculated from the *s*- and *p*-polarized signals simultaneously collected by a lock-in amplifier. All reported IR spectra were repeated at least twice using independent sample preparations.

Film coverage and surface morphology were investigated with an Olympus BX41 microscope with Pixera camera and Pixera Viewfinder Pro imaging software. Ellipsometric thicknesses were determined from a J.A. Woollam M-2000DI variable angle spectroscopic ellipsometer. Thicknesses were fit to data taken at 75° from the surface normal over wavelengths from 400 to 700 nm, using a refractive index of 1.53[41,42] for polynorbornene and 1.47 for sulfonated polynorbornene, accounting for a 0.06 decrease in the refractive index of the sulfated films because of the optical properties imparted by the sulfonate group.[43] Optical constants of the underlying gold used in the preparation of each sample were taken prior to polymer film deposition and used as a baseline for thickness measurements. Reported thickness values and errors represent the averages and standard deviations, respectively, from at least six different films.

Contact angles of water were measured with a Rame-Hart manual contact angle goniometer. Advancing and receding contact angle measurements were taken on both sides of ~5 μL drops of water with the microliter syringe tip remaining inside the drop during measurement. Reported values and errors represent the averages and standard deviations, respectively, from at least six different films.

Proton Conductivity Study. Electrochemical impedance spectroscopy (EIS) was performed with a Gamry Instruments CMS300 impedance system interfaced to a personal computer. A flat cell (EG&G) was used to selectively expose 1.0 cm^2 of each sample as the working electrode to an aqueous solution of 0.1 M H_2SO_4. Measurements were taken using a Ag/AgCl/saturated KCl reference electrode with evaporated gold on silicon as the counter electrode. Data were collected between 10^{-1} and 10^5 Hz and fit using appropriate equivalent circuits[44,45] to determine film resistance, film capacitance, and interfacial capacitance values, where applicable. Data collected between 10^4 and 10^5 Hz were omitted from the analysis due to inductive interference. Reported values and errors represent the averages and standard deviations, respectively, from at least six different films.

Results and Discussion

Growth of Surface-Initiated Polynorbornene. The exposure of a gold-coated silicon substrate to an ethanolic solution of 4-mercapto-1-butanol results in a thin, hydroxyl-terminated SAM on gold. The high surface energy ($\theta_A(H_2O) \approx 36°$) of the SAM surface is consistent with that of a thin hydroxyl-terminated SAM. Hydroxyl-terminated SAMs on gold with six or fewer carbons in the alkyl backbone have been shown to exhibit a unique striped structure driven by intermolecular hydrogen bonding.[46] The striped structure leads to films that are thinner and of a more intermediate surface energy than predicted by the trans-extended, canted structure known to SAMs on gold with 10 or more carbons in the alkyl backbone.[47−50] The combination of the thin structure of the SAM and the typical adventitious layer of carbon on a bare gold substrate[49] results in the inability to ellipsometrically distinguish the SAM monolayer from the gold background. Nonetheless, the presence of this SAM is required to anchor the norbornenyl group and initiate polymerization (vide infra), as no polymer is grown when this step is omitted.

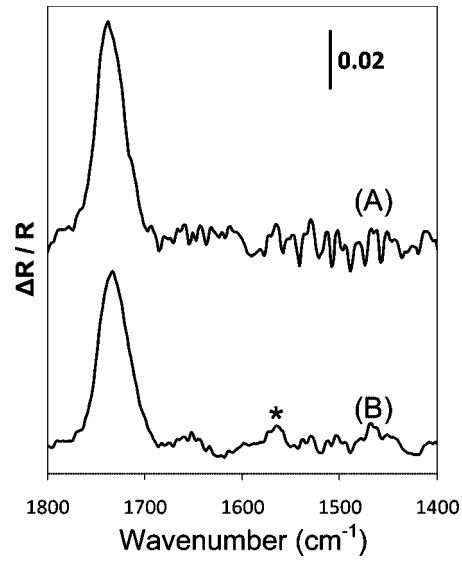

Figure 2. PM-IRRAS spectra of norbornenyl-capped monolayers exposed to (A) ethanol or (B) water. The asterisk (∗) denotes a weak peak at 1560 cm^{-1} due to carbonyl stretching of the carboxylate group.

The immobilization of norbornenyl functionality is accomplished by exposure of the hydroxyl-terminated SAM to trans-3,6-endomethylene-1,2,3,6-tetrahydrophthaloyl chloride ($NB(COCl)_2$) in dichloromethane. The increase in the advancing water contact angle ($\theta_A(H_2O) \approx 59°$) over that of the SAM ($\theta_A(H_2O) \approx 36°$) is consistent with the introduction of an incomplete adlayer of norbornenyl groups on a hydroxyl surface. $NB(COCl)_2$ can attach to the hydroxyl surface by reacting to produce one or two ester linkages. We investigated the multiplicity of $NB(COCl)_2$ attachment to the monolayer via observation of ester formation using PMIRRAS. Immediately after the exposure to $NB(COCl)_2$, the films were rinsed with water for 30 s to hydrolyze the acid chloride of any norbornenyl groups only tethered by one ligand. As a control, separate samples were rinsed with ethanol to react with untethered acid chloride to form ethyl esters. In the IR spectrum, carbonyl stretching due to carboxylate ($\nu_{C=O} \approx 1560$ cm^{-1}) and carboxylic acid ($\nu_{C=O} \approx 1710$ cm^{-1}) functionality is differentiated from that due to ester ($\nu_{C=O} \approx 1735$ cm^{-1}) functionality,[23,44,51,52] allowing a relative determination of the multiplicity of norbornenyl attachment through peak area integration. The IR spectra of the water-rinsed samples (Figure 2B) indicate additional carboxylate functionality at 1560 cm^{-1}. The IR spectra of ethanol-rinsed samples (Figure 2A) show a lower signal-to-noise ratio while indicating a lack of carboxylate functionality at 1560 cm^{-1}. Assuming similar extinction coefficients and average orientations for carboxylate and ester carbonyl functionality, integration of peak areas for the carbonyl stretching due to ester (A_{ester}) and carboxylate ($A_{carboxylate}$) functionality allows an estimation of the mean multiplicity (m) of norbornenyl attachment using

$$m = \frac{A_{ester} - \frac{A_{ester} + A_{carboxylate}}{2}}{\frac{A_{ester} + A_{carboxylate}}{2}} + 1 \qquad (1)$$

Table 1. Advancing and Receding Water Contact Angles for Specified Films

film	θ_A(water) (deg)	θ_R(water) (deg)
$-SC_4OH$ SAM	36 ± 1	<10
NB-decorated SAM	59 ± 2	12 ± 6
catalyst-decorated SAM	62 ± 1	17 ± 4
pNB	101 ± 1	74 ± 4
sulfonated pNB	75 ± 7	<10

The majority (~90%, $m \approx 1.9$) of the norbornenyl groups were attached via two ester bonds to the underlying monolayer. The resulting two ester attachment to the monolayer is similar to a chelated system and should improve the stability of the bound species.[53,54]

The norbornenyl decorated surface was exposed to Grubbs first-generation catalyst to activate the surface for ROMP. Evidence of successful attachment of the catalyst includes a ~5 Å increase in ellipsometric thickness and successful polymerization (vide infra), but the contact angle of water on the surface of the film was barely changed from the norbornenyl-terminated surface (Table 1). Immersion of the catalyst-coated substrate in a solution of 1.0 M norbornene in toluene for 15 min results in a ~120 nm thick, surface-tethered film of ROMP-type polynorbornene. Surface-initiated polynorbornene films have been previously characterized by us[31] and others.[21,55] We will only highlight physical and chemical properties of polynorbornene relevant to this study. The advancing water contact angle ($\theta_A(H_2O) \approx 101°$) is consistent with a hydrocarbon surface.[31,50] The RAIRS spectra of polynorbornene (Figure 3A) clearly shows crisp and intense asymmetric and symmetric CH_2 (2948 and 2866 cm^{-1}) and CH stretching (2911 cm^{-1}) peaks. The position of the CH_2 scissoring peak (~1450 cm^{-1}) is indicative of purely cyclic CH_2 functionality.[56] The olefin functionality is observed in the trans C═CH out of plane bending[35,56] peak (968 cm^{-1}).

Sulfonation of Polynorbornene. Upon subsequent exposure of the polynorbornene film (Figure 3A) to 0.1 M acetyl sulfate for 1 min and to DMSO for 30 min (Figure 3C), the RAIR spectrum indicates ~95% reduction of the trans C═CH out of plane bending peak (968 cm^{-1}) and reduction of all peaks associated with olefin functionality. The introduction of protonated sulfonate functionality is observed through the appearance of asymmetric and symmetric SO_3 stretching (~1343 and ~1167 cm^{-1}, respectively) and S-OH stretching (923 cm^{-1}) modes.[35,56,57] The corresponding asymmetric and symmetric SO_3 stretching modes for the deprotonated species are also observed in the spectrum for the sulfonated film at ~1201 and ~1040 cm^{-1}, respectively.[58] The C═CH out of plane bending peak at 810 cm^{-1} associated with the olefinic sulfonate product[35] is not present, indicating the preferential formation of the hydroxyl-sulfonate product. The resulting hydroxylsulfonate eliminates the unsaturation of the backbone, improving the chemical stability of the polymer film (vide infra). The introduction of the hydroxyl functionality, observed as a broad peak from 3700 to 3100 cm^{-1}, is further evidence of the hydroxylsulfonate product. The decrease in olefin functionality coupled with an increase in all modes associated with sulfonate and hydroxyl functionality is consistent with the conversion of the olefin to the hydroxylsulfonate product. The position of the CH_2 scissoring peak (~1450 cm^{-1}) is indicative of the conservation of the cyclic CH_2 functionality after sulfonation.[56] The crisp asymmetric and symmetric CH_2 (2948 and 2866 cm^{-1}) and CH stretching (2911 cm^{-1}) peaks of the polynorbornene spectrum[21] are reduced and distorted upon sulfonation. While it is common for the intensities[21,59] and positions[60] of peaks in the RAIR spectrum to be altered as the chains reorganize, the complementary decrease in ellipsometric film thickness during sulfonation from 120 to 71 nm indicates a ~41% loss of polymer chains from the film. Literature provides no record of or mechanism for chain scission at the olefin site during sulfonation.[33−36,40]

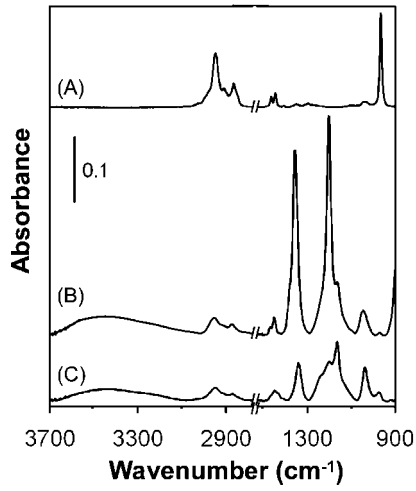

Figure 3. Reflectance-absorption infrared spectra of surface-initiated polynorbornene (A) and sulfonated polynorbornene before (B) and after (C) a 30 min exposure to DMSO. The spectra have been offset vertically for clarity.

Table 2. Percentage Film Losses for a Typical Preparation of Sulfonated Polynorbornene (see Figure 1) and for Three Controls Where No Sulfonation Agent Was Used

condition	typical	control I	control II	control III
acetyl sulfate present?	yes	no	no	no
thiolate linkage?	yes	yes	no	no
ester linkage?	yes	yes	no	no
DMSO soak?	yes	yes	no	no
catalyst quenched?	no	no	no	yes
% loss	41 ± 32	34 ± 23	45 ± 13	44 ± 17

To further explore the loss of film during sulfonation, we performed a series of controls, numbered I through III in Table 2. To test if sulfonation was causing chain scission (control I), the same procedure was performed without a sulfonating agent (acetyl sulfate) as a blank control. Film thicknesses of the polymer samples decreased $34 \pm 22\%$ during the blank controls to indicate that the majority of film loss, if not all, is independent of exposure to acetyl sulfate. To test if the film was being cleaved at the thiolate linkage to the Au substrate, polymer was grown from a silicon surface using a more stable 7-octenyl trichlorosilane linkage (Control II). This strategy also eliminates the ester linkage that binds the norbornenyl group in our typical approach, shown in Figure 1. Film thicknesses on the silane-bound polymer films decreased $45 \pm 13\%$ upon exposure to dichloromethane (no acetyl sulfate) to indicate the film loss is also independent of the polymer/substrate linkage. As further evidence that the thiolate linkage is stable to sulfonation, we exposed a self-assembled monolayer derived from *n*-pentanethiol to the sulfonation conditions for 5 min (rather than 1 min in our typical sulfonation) and observed that its contact angle and impedance properties were unaffected. Several mechanisms are potentially responsible for cleavage of the polynorbornene prior to sulfonation, including secondary metathesis.[24,31,61] Secondary metathesis refers to the reaction of the metathesis catalyst with the olefin functionality in the repeat unit of a ROMP-type polymer, cleaving the polymer chain.[61] Exposure of the polynorbornene films prior to removal from the polymerization

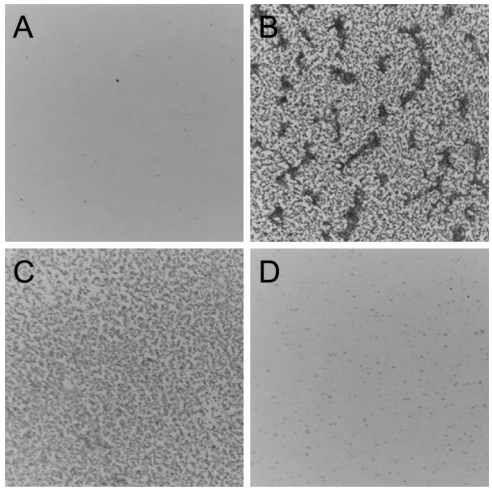

Figure 4. Optical microscope images (250 μm × 250 μm) of surface-initiated polynorbornene before sulfonation (A), after sulfonation (B), and sulfonated polynorbornene after 5 min (C) and 30 min (D) exposure to DMSO.

bath (control III) to ethyl vinyl ether, an agent used to terminate the catalytic activity in Grubbs catalysts, resulted in no reduction in ellipsometric film loss (44 ± 17%) upon exposure to dichloromethane, suggesting that secondary metathesis is not the primary mechanism for film loss. Since the controls suggest that the film loss is not due to the sulfonation agent, the polymer/substrate linkage, or secondary metathesis activity, the film loss likely occurs at the olefin sites in the polymer backbone such that the cleaved chain fragments are pulled from the surface into solvent during rinsing or further processing steps. Polymers with internal olefins are known to be unstable to heat[62] and oxidizing conditions,[63] but the literature does not address the stability of polynorbornene films to common solvents under ambient conditions. If the olefin sites are indeed responsible for the poor stability of the film in common solvents, then the sulfonated film should be more robust since the olefins are converted to hydroxylsulfonates (Figure 1D).

Inspection of the polynorbornene films immediately after exposure to acetyl sulfate through optical microscopy (Figure 4B) reveals a nonuniform surface with polymer aggregates. These aggregates were shown via atomic force microscopy to be in excess of 500 nm tall for a film with an ellipsometric thickness of only ~70 nm. This unique surface morphology is a result of the contrasting solvation behavior of polynorbornene and sulfonated polynorbornene. During sulfonation, the polynorbornene chains are well solvated and likely stretched away from the substrate in dicholoromethane,[33,64] but the sulfonation product is not well solvated in dichloromethane.[33] As the reaction proceeds, the sulfonated polynorbornene forms insoluble clusters of chains that are extended away from the surface, resulting in a highly nonuniform surface morphology. Through exposure to DMSO, a good solvent for sulfonated polynorbornenes,[33] the polymer chains relax into a less constrained conformation, providing a more uniform surface morphology (Figure 4C,D). As the polymer relaxes, the average orientation of the backbone becomes less normal to the surface, and the average orientation of the sulfonate groups becomes more normal to the surface. This shift in orientation results in the SO_3 asymmetric stretching being less aligned with the RAIR-induced electric field normal to the surface. As a result, the relaxation of the sulfonated ionomer film is observed in the RAIR spectra (Figure 3B,C) through diminution of the asymmetric SO_3 stretching modes of the protonated and deprotonated

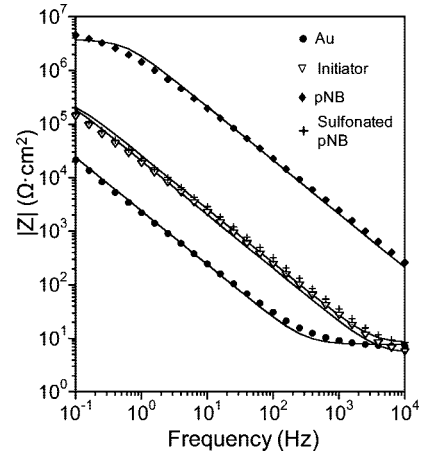

Figure 5. Electrochemical impedance spectra obtained in 0.1 M H_2SO_4 (aq) for the indicated films on gold. Solid curves represent fits of the data using appropriate equivalent circuit models.

Table 3. Film Resistance and Interfacial Capacitance for Indicated Films

film	log (R_f) ($\Omega \cdot cm^2$)	C_i (μF)
bare gold	[a]	63.4 ± 3.6
NB decorated SAM	[a]	7.3 ± 1.1
pNB	6.5 ± 0.8	[b]
sulfonated pNB	0.21 ± 0.11	6.6 ± 0.7

[a] These systems are not modeled with a film resistance.[45] [b] Beyond measurable range of instrument.

state (1343 and 1201 cm^{-1}, respectively). Most importantly, the exposure of the sulfonated films to DMSO resulted in no reduction in symmetric SO_3 stretching modes (1167 and 1040 cm^{-1}) or CH stretching modes (2800−3000 cm^{-1}), indicating the stability of the sulfonated film. Because of the replacement of olefins by hydroxylsulfonates during sulfonation, the resulting sulfonated polynorbornene films are far more stable than the polynorbornene films and show no loss in film thickness upon aggressive rinsing with ethanol and DMSO after one week in ambient laboratory conditions or upon exposure to O_2-saturated aqueous solutions containing 0.1 M H_2SO_4 that are more representative of a fuel cell environment. Nonetheless, further testing will be required before the films are investigated for such applications.

Proton Conduction in Sulfonated Polynorbornene Films. We used electrochemical impedance spectroscopy (EIS) with a 0.1 M H_2SO_4 (aq) electrolyte solution to probe the resistance of the polymer films against proton transport. Characteristic impedance spectra in the form of Bode plots for the gold-coated substrate, the NB-decorated monolayer (initiator), a ~120 nm polynorbornene film, and a ~71 nm sulfonated polynorbornene film after a 30 min exposure to DMSO are shown in Figure 5. Values of film resistance (R_f) and interfacial capacitance (C_i) were determined by fits to equivalent circuit models[44,45] and are provided in Table 3. Since no redox active species are present in the electrolyte, the bare gold electrode and the NB-modified SAM are modeled by a solution resistance in series with an interfacial capacitance. The equivalent circuit used to model the polymer films[44] is more complex, but both are shown in Figure S1 in the Supporting Information.

Modification of the gold electrode by the NB-modified SAM results in an increase in impedance at intermediate frequencies that corresponds to the reduced interfacial capacitance imparted by the SAM (Table 3). The spectrum for polynorbornene is 2 orders of magnitude higher in impedance than the SAM and

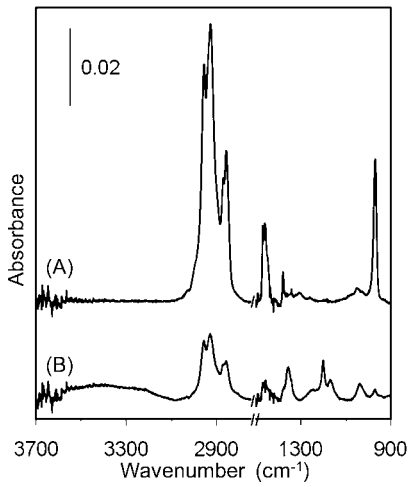

Figure 6. Reflectance−absorption infrared spectra of surface-initiated poly(*n*-butylnorbornene) before (A) and after sulfonation (B). The spectra have been offset vertically for clarity.

consists of a well-defined capacitive region ($C_f = 110 \pm 50$ nF) at intermediate frequencies and a resistive region ($R_f \approx 10^{6.5}$ $\Omega \cdot cm^2$) at low frequencies, both associated with the polymer film, and are comparable to those observed previously by us using $K_3Fe(CN)_6$ and $K_4Fe(CN)_6$ as redox probes.[31] This film provides a large barrier against the transport of protons and other aqueous ions. Upon sulfonation and exposure to DMSO, the spectrum of the sulfonated polymer film nearly overlays that of the initiator SAM, indicating an extremely low resistance against proton transfer ($\sim$1.6 $\Omega \cdot cm^2$). This film resistance is 5 orders of magnitude lower than that of polynorbornene and is only evident at the highest frequencies as a plateau that is slightly higher than that due to the solution resistance of the SAM. The interfacial capacitance, which probes the nature of the gold/organic interface, is comparable for the initiator ($C_i \approx$ 7.3 μF) and sulfonated polynorbornene ($C_i \approx 6.6$ μF), while the interfacial capacitance of the polynorbornene film is obscured in the available frequency range by the large impedance due to the film. Exposure of the sulfonated polynorbornene to DMSO has a negligible effect on the impedance properties of the film (comparison not shown for figure clarity). The low resistance to proton transfer in the sulfonated polynorbornene is encouraging for future investigation into these ionomer-modified interfaces.

Sulfonation of Poly(*n*-butylnorbornene). To demonstrate the versatility of this approach toward sulfonated films, we prepared and sulfonated surface-initiated poly(butylnorbornene) in a manner analogous to that of the polynorbornene films (Figure 1). These films were also exposed to DMSO for 30 min, in a manner consistent with polynorbornene samples. The reaction of poly(butylnorbornene) with acetyl sulfate was monitored via RAIRS (Figure 6). The IR spectrum of poly(butylnorbornene) is thoroughly described in our previous work.[31] Exposure to acetyl sulfate reduced the peak area corresponding to trans C=CH out of plane bending (968 cm^{-1}) by over 96%. Asymmetric and symmetric SO_3 stretching peaks at 1355 and 1168 cm^{-1}, respectively, indicate the additional sulfonate functionality.[35,56,57] The corresponding asymmetric and symmetric stretching modes for the deprotonated species are located at $\sim$1200 and $\sim$1038 cm^{-1}, respectively.[58] The C=CH out of plane bending peak at 810 cm^{-1} associated with the olefinic sulfonate product[35] is not present indicating the preferential formation of the hydroxysulfonate product. The cyclic and linear CH_2 stretching modes are reduced and shifted 1−2 cm^{-1} toward higher wavenumbers, indicative of a disruption of the original methylene packing.[47] The sulfonation of poly(butylnorbornene) exhibits similar film loss to that observed in the polynorbornene system. The ratio of total methylene functionality (3000−2800 cm^{-1}) to sulfonate functionality is higher in the sulfonated poly(butylnorbornene) films than the sulfonated polynorbornene films because of the additional butyl side chain. Sulfonated poly(butylnorbornene) films exhibit a higher surface energy ($\theta_A(H_2O) = 95 \pm 2°$) than that of the original poly(butylnorbornene) film ($\theta_A(H_2O) = 109 \pm 2°$), but the additional butyl functionality increases surface hydrophobicity beyond that measured on sulfonated polynorbornene ($\theta_A(H_2O) \approx 75°$).

Conclusions

Surface-tethered sulfonated polymer films are easily prepared through the exposure of excess acetyl sulfate to surface-initiated polynorbornene films. The sulfonated films are thinner than their polynorbornene precursors, due to some chain loss that is independent of the sulfonation reagent or the mode of surface attachment and likely occurs at the olefin sites in the polynorbornene chain backbone. Sulfonation of surface-initiated polynorbornene greatly diminishes the olefin content in the film and results in a much more stable film. The sulfonated film initially exhibits a highly nonuniform surface morphology which can be relaxed to a more uniform surface through exposure to DMSO. Sulfonated polynorbornene films have an intermediate surface energy, and the film resistance to proton transfer due to the sulfonated polymer is very small. The ability to generate sulfonated films from functional polynorbornenes is demonstrated through the sulfonation of poly(butylnorbornene). We have also highlighted a novel approach toward a norbornenyl-decorated SAM for the immobilization of a metathesis catalyst on a surface. The ability to create uniform sulfonated films on complex geometries has potential application in high surface area electrode assemblies, which we will highlight in a subsequent manuscript.

Acknowledgment

The project was supported by the U.S. Department of Energy (ER46239). The authors thank Dr. Ed Elce (Promerus Electronic Materials) for generously providing the *n*-butylnorbornene monomer. B.J.B. thanks the Vanderbilt Institute of Nanoscale Science and Engineering for a fellowship. P.A.P. thanks the Vanderbilt Undergraduate Summer Research Program for funding. We thank Professor Bridget Rogers for the use of the ellipsometer.

Supporting Information Available: A presentation and discussion of the equivalent circuit models used to analyze electrochemical impedance spectra are provided. This material is available free of charge via the Internet at http://pubs.acs.org.

Literature Cited

(1) Carrette, L.; Friedrich, K. A.; Stimming, U. Fuel Cells: Principles, Types, Fuels, and Applications. *ChemPhysChem* **2000**, *1*, 162–193.

(2) Iojoiu, C.; Marechal, M.; Chabert, F.; Sanchez, J. Y. Mastering Sulfonation of Aromatic Polysulfones: Crucial for Membranes for Fuel Cell Application. *Fuel Cells* **2005**, *5*, 344–354.

(3) Jinnouchi, R.; Okazaki, K. Molecular Dynamics Study of Transport Phenomena in Perfluorosulfonate Ionomer Membranes for Polymer Electrolyte Fuel Cells. *J. Electrochem. Soc.* **2003**, *150*, E66–E73.

(4) Roziere, J.; Jones, D. J. Non-Fluorinated Polymer Materials for Proton Exchange Membrane Fuel Cells. *Annu. Rev. Mater. Res.* **2003**, *33*, 503–555.

(5) Saito, M.; Arimura, N.; Hayamizu, K.; Okada, T. Mechanisms of Ion and Water Transport in Perfluorinated Ionomer Membranes for Fuel Cells. *J. Phys. Chem. B* **2004**, *108*, 16064–16070.

(6) Carrette, L.; Friedrich, K. A.; Stimming, U. Fuel Cells: Principles, Types, Fuels, and Applications. *ChemPhysChem* **2000**, *1*, 162–193.

(7) Middelman, E. Improved PEM Fuel Cell Electrodes by Controlled Self-Assembly. *Fuel Cells Bull.* **2002**, *11*, 9–12.

(8) Litster, S.; McLean, G. PEM Fuel Cell Electrodes. *J. Power Sources* **2004**, *130*, 61–76.

(9) Cha, S. W.; O'Hayre, R.; Prinz, F. B. The Influence of Size Scale on the Performance of Fuel Cells. *Solid State Ionics* **2004**, *175*, 789–795.

(10) Cha, S. Y.; Lee, W. M. Performance of Proton Exchange Membrane Fuel Cell Electrodes Prepared by the Direct Deposition of Ultrathin Platinum on the Membrane Surface. *J. Electrochem. Soc.* **1999**, *146*, 4055–4060.

(11) Lux, K. W.; Rodriguez, K. J. Template Synthesis of Arrays of Nano Fuel Cells. *Nano Lett.* **2006**, *6*, 288–295.

(12) Zeis, R.; Mathur, A.; Fritz, G.; Lee, J.; Erlebacher, J. Platinum-Plated Nanoporous Gold: An Efficient, Low Pt Loading Electrocatalyst for PEM Fuel Cells. *J. Power Sources* **2007**, *165*, 65–72.

(13) Hinkebein, T. E.; Price, M. K. Progress with the Desalination and Water Purification Technologies U.S. Roadmap. *Desalination* **2005**, *182*, 19–28.

(14) Nagarale, R. K.; Gohil, G. S.; Shahi, V. K. Recent Developments on Ion-Exchange Membranes and Electro-Membrane Processes. *Adv. Colloid Interface Sci.* **2006**, *119*, 97–130.

(15) Eckenrode, H. M.; Dai, H. L. Nonlinear Optical Probe of Biopolymer Adsorption on Colloidal Particle Surface: Poly-L-lysine on Polystyrene Sulfate Microspheres. *Langmuir* **2004**, *20*, 9202–9209.

(16) Hesselink, F. T. *Adsorption Form Solution at the Solid/Liquid Interface*; Academic Press: New York, 1983.

(17) Ramstedt, M.; Cheng, N.; Azzaroni, O.; Mossialos, D.; Mathieu, H. J.; Huck, W. T. S. Synthesis and Characterization of Poly(3-sulfopropylmethacrylate) Brushes for Potential Antibacterial Applications. *Langmuir* **2007**, *23*, 3314–3321.

(18) Jennings, G. K.; Brantley, E. L. Physicochemical Properties of Surface-Initiated Polymer Films in the Modification and Processing of Materials. *Adv. Mater.* **2004**, *16*, 1983–1994.

(19) Bantz, M. R.; Brantley, E. L.; Weinstein, R. D.; Moriarty, J.; Jennings, G. K. Effect of Fractional Fluorination on the Properties of ATRP Surface-Initiated Poly(hydroxyethyl methacrylate) Films. *J. Phys. Chem. B* **2004**, *108*, 9787–9794.

(20) Kim, J.-B.; Huang, W.; Bruening, M. L.; Baker, G. L. Synthesis of Triblock Copolymer Brushes by Surface-Initiated Atom Transfer Radical Polymerization. *Macromolecules* **2002**, *35*, 5410–5416.

(21) Kim, N. Y.; Jeon, N. L.; Choi, I. S.; Takami, S.; Harada, Y.; Finnie, K. R.; Girolami, G. S.; Nuzzo, R. G.; Whitesides, G. M.; Laibinis, P. E. Surface-Initiated Ring-Opening Metathesis Polymerization on Si/SiO_2. *Macromolecules* **2000**, *33*, 2793–2795.

(22) Matyjaszewski, K.; Miller, P. J.; Shukla, N.; Immaraporn, B.; Gelman, A.; Luokala, B. B.; Siclovan, T. M.; Kickelbick, G.; Vallant, T.; Hoffmann, H.; Pakula, T. Polymers at Interfaces: Using Atom Transfer Radical Polymerization in the Controlled Growth of Homopolymers and Block Copolymers from Silicon Surfaces in the Absence of Untethered Sacrificial Initiator. *Macromolecules* **1999**, *32*, 8716–8724.

(23) Bai, D.; Hardwick, C. L.; Berron, B. J.; Jennings, G. K. Kinetics of pH Response for Copolymer Films with Dilute Carboxylate Functionality. *J. Phys. Chem. B* **2007**, *111*, 11400–11406.

(24) Jordi, M. A.; Seery, T. A. P. Quantitative Determination of the Chemical Composition of Silica−Poly(norbornene) Nanocomposites. *J. Am. Chem. Soc.* **2005**, *127*, 4416–4422.

(25) Watson, K. J.; Zhu, J.; Nguyen, S. T.; Mirkin, C. A. Hybrid Nanoparticles with Block Copolymer Shell Structures. *J. Am. Chem. Soc.* **1999**, *121*, 462–463.

(26) Harada, Y.; Girolami, G. S.; Nuzzo, R. G. Catalytic Amplification of Patterning Via Surface-Confined Ring-Opening Metathesis Polymerization on Mixed Primer Layers Formed by Contact Printing. *Langmuir* **2003**, *19*, 5104–5114.

(27) Liu, X. G.; Guo, S. W.; Mirkin, C. A. Surface and Site-Specific Ring-Opening Metathesis Polymerization Initiated by Dip-Pen Nanolithography. *Angew. Chem., Int. Ed.* **2003**, *42*, 4785–4789.

(28) Lee, W. K.; Caster, K. C.; Kim, J.; Zauscher, S. Nanopatterned Polymer Brushes by Combining AFM Anodization Lithography with Ring-Opening Metathesis Polymerization in the Liquid and Vapor Phase. *Small* **2006**, *2*, 848–853.

(29) Voronov, A.; Shafranska, O. Synthesis of Chemically Grafted Polystyrene "Brushes" And Their Influence on the Dewetting in Thin Polystyrene Films. *Langmuir* **2002**, *18*, 4471–4477.

(30) Husseman, M.; Malmstrom, E. E.; McNamara, M.; Mate, M.; Mecerreyes, D.; Benoit, D. G.; Hedrick, J. L.; Mansky, P.; Huang, E.; Russell, T. P.; Hawker, C. J. Controlled Synthesis of Polymer Brushes By "Living" Free Radical Polymerization Techniques. *Macromolecules* **1999**, *32*, 1424–1431.

(31) Berron, B. J.; Graybill, E. P.; Jennings, G. K. Growth and Structure of Surface-Initiated Poly(*N*-alkylnorbornene) Films. *Langmuir* **2007**, *23*, 11651–11655.

(32) Mizuhata, H.; Nakao, S.; Yamaguchi, T. Morphological Control of PEMFC Electrode by Graft Polymerization of Polymer Electrolyte onto Platinum-Supported Carbon Black. *J. Power Sources* **2004**, *138*, 25–30.

(33) Boyd, T. J.; Schrock, R. R. Sulfonation and Epoxidation of Substituted Polynorbornenes and Construction of Light-Emitting Devices. *Macromolecules* **1999**, *32*, 6608–6618.

(34) Gilbert, E. E. *Sulfonation and Related Reactions*; John Wiley & Sons Inc.: New York, 1965.

(35) Planche, J. P.; Revillon, A.; Guyot, A. Chemical Modification of Polynorbornene. 1. Sulfonation in Dilute Solution. *J. Polym. Sci., Part A* **1988**, *26*, 429–444.

(36) Planche, J. P.; Revillon, A.; Guyot, A. Chemical Modification of Polynorbornene. 2. Extended Sulfonation Processes. *J. Polym. Sci., Part A* **1990**, *28*, 1377–1386.

(37) Hofmann, K.; Simchen, G. Sulfosilylation of Carbonyl-Compounds and a Simple Synthesis of Sulfur-Trioxide-1,4-Dioxane-Adducts and Sulfur-Trioxide-1,4-Pyridine-Adducts. *Synthesis (Stuttgart)* **1979**, *9*, 699–700.

(38) Wuts, P. G. M.; Wilson, K. E. Trimethylsilyl Directed Aromatic Sulfonation with Sulfur Trioxide−Dioxane Complex. *Synthesis (Stuttgart)* **1998**, *11*, 1593–1595.

(39) Tran, Y.; Auroy, P. Synthesis of Poly(styrene sulfonate) Brushes. *J. Am. Chem. Soc.* **2001**, *123*, 3644–3654.

(40) Bakker, B. H.; Cerfontain, H. Aliphatic Sulfonation. 16 - Sulfonation of Alkenes by Chlorosulfuric Acid, Acetyl Sulfate, and Trifluoroacetyl Sulfate. *Eur. J. Org. Chem.* **1999**, *1*, 91–96.

(41) Nikolov, I. D.; Ivanov, C. D. Optical Plastic Refractive Measurements in the Visible and the Near-Infrared Regions. *Appl. Opt.* **2000**, *39*, 2067–2070.

(42) Shin, J. Y.; Park, J. Y.; Liu, C. Y.; He, J. S.; Kim, S. C. Chemical Structure and Physical Properties of Cyclic Olefin Copolymers (IUPAC Technical Report). *Pure Appl. Chem.* **2005**, *77*, 801–814.

(43) Jung, S. D.; Hwang, W. Y.; Song, S. H.; Lee, E. H.; Lee, J. I.; Shim, H. K. Sulfonated Polystyrene as a New Gradient-Index Medium for Light-Focusing Elements. *Opt. Lett.* **1995**, *20*, 1236–1237.

(44) Bai, D. S.; Habersberger, B. M.; Jennings, G. K. pH-Responsive Copolymer Films by Surface-Catalyzed Growth. *J. Am. Chem. Soc.* **2005**, *127*, 16486–16493.

(45) Nahir, T. M.; Bowden, E. F. Impedance Spectroscopy of Electroinactive Thiolate Films Adsorbed on Gold. *Electrochim. Acta* **1994**, *39*, 2347–2352.

(46) Tsukamoto, K.; Kubo, T.; Nozoye, H. Structure of Mercaptoalcohol Self-Assembled Monolayers on Au(111). *Appl. Surf. Sci.* **2005**, *244*, 578–583.

(47) Berron, B.; Jennings, G. K. Loosely Packed Hydroxyl-Terminated Sams on Gold. *Langmuir* **2006**, *22*, 7235–7240.

(48) Porter, M. D.; Bright, T. B.; Allara, D. L.; Chidsey, C. E. D. Spontaneously Organized Molecular Assemblies. 4. Structural Characterization of Normal-Alkyl Thiol Monolayers on Gold by Optical Ellipsometry, Infrared-Spectroscopy, and Electrochemistry. *J. Am. Chem. Soc.* **1987**, *109*, 3559–3568.

(49) Bain, C. D.; Troughton, E. B.; Tao, Y. T.; Evall, J.; Whitesides, G. M.; Nuzzo, R. G. Formation of Monolayer Films by the Spontaneous Assembly of Organic Thiols from Solution onto Gold. *J. Am. Chem. Soc.* **1989**, *111*, 321–335.

(50) Laibinis, P. E.; Palmer, B. J.; Lee, S.-W.; Jennings, G. K. The Synthesis of Organothiols and Their Assembly into Monolayers on Gold. In *Thin Films*; Ulman, A., Ed.; Academic Press: Boston, MA, 1998.

(51) Bai, D.; Jennings, G. K. Surface-Catalyzed Growth of Polymethylene-Rich Copolymer Films on Gold. *J. Am. Chem. Soc.* **2005**, *127*, 3048–3056.

(52) Bai, D. S.; Elliott, S. M.; Jennings, G. K. pH-Responsive Membrane Skins by Surface-Catalyzed Polymerization. *Chem. Mater.* **2006**, *18*, 5167–5169.

(53) Park, J. S.; Vo, A. N.; Barriet, D.; Shon, Y. S.; Lee, T. R. Systematic Control of the Packing Density of Self-Assembled Monolayers Using Bidentate and Tridentate Chelating Alkanethiols. *Langmuir* **2005**, *21*, 2902–2911.

(54) Shon, Y. S.; Lee, T. R. Desorption and Exchange of Self-Assembled Monolayers on Gold Generated from Chelating Alkanedithiols. *J. Phys. Chem. B* **2000**, *104*, 8192–8200.

(55) Rutenberg, I. M.; Scherman, O. A.; Grubbs, R. H.; Jiang, W.; Garfunkel, E.; Bao, Z. Synthesis of Polymer Dielectric Layers for Organic

Thin Film Transistors Via Surface-Initiated Ring-Opening Metathesis Polymerization. *J. Am. Chem. Soc.* **2004**, *126*, 4062–4063.

(56) Silverstein, R.; Webster, F.; Kiemle, D. *Spectrometric Identification of Organic Compounds*, 7th ed.; John Wiley & Sons Inc.: New York, 2005.

(57) Langner, R.; Zundel, G. FT-IR Investigation of Polarizable, Strong Hydrogen-Bonds in Sulfonic-Acid-Sulfoxide, Sulfonic-Acid-Phosphine-Oxide, and Sulfonic-Acid-Arsine-Oxide Complexes in the Middle-Infrared and Far-Infrared Region. *J. Phys. Chem.* **1995**, *99*, 12214–12219.

(58) Bellamy, L. J. The Infrared Spectra of Organo Sulfur Compounds. In *Organic Sulfur Compounds*; Kharasch, N., Ed.; Pergamon Press: New York, 1961.

(59) Nuzzo, R. G.; Dubois, L. H.; Allara, D. L. Fundamental-Studies of Microscopic Wetting on Organic-Surface. 1. Formation and Structural Characterization of a Self-Consistent Series of Polyfunctional Organic Monolayers. *J. Am. Chem. Soc.* **1990**, *112*, 558–569.

(60) Weinstein, R. D.; Moriarty, J.; Cushnie, E.; Colorado, R.; Lee, T. R.; Patel, M.; Alesi, W. R.; Jennings, G. K. Structure, Wettability, and Electrochemical Barrier Properties of Self-Assembled Monolayers Prepared from Partially Fluorinated Hexadecanethiols. *J. Phys. Chem. B* **2003**, *107*, 11626–11632.

(61) Lynn, D. M.; Kanaoka, S.; Grubbs, R. H. Living Ring-Opening Metathesis Polymerization in Aqueous Media Catalyzed by Well-Defined Ruthenium Carbene Complexes. *J. Am. Chem. Soc.* **1996**, *118*, 784–790.

(62) Otsuki, T.; Goto, K.; Komiya, Z. Development of Hydrogenated Ring-Opening Metathesis Polymers. *J. Polym. Sci.* **2000**, *38*, 4661–4668.

(63) Shiono, T.; Yoshino, O.; Ikeda, T. Synthesis and Oxidative Degradation of Poly(ethene-ran-1,3-butadiene). *Macromol. Rapid Commun.* **2000**, *21*, 1297–1301.

(64) Bielawski, C. W.; Grubbs, R. H. Increasing the Initiation Efficiency of Ruthenium-Based Ring-Opening Metathesis Initiators: Effect of Excess Phosphine. *Macromolecules* **2001**, *34*, 8838–8840.

Received for review March 04, 2008
Revised manuscript received August 7, 2008
Accepted August 12, 2008

IE800356A